

Chapter 7

Barker-Fisher-Watts fluid: its power exponents and fluid-solid boundary

In Chapter 5 we demonstrated that in the case of the Lennard-Jones fluid, the viscosity, pressure and energy exponents are not fixed values. They depend on state point, namely, the temperature and density. We gave the results of simulations for the exponents varying with temperature and density, and we also found that the relationship can be expressed easily by a linear function of both temperature and density. In Chapter 6, we found a method with which one can use a combination of equilibrium and nonequilibrium molecular dynamics to determine the fluid-solid boundary for the Lennard-Jones fluid. Our results agreed with those of other workers.

In this chapter, we will consider using the Barker-Fisher-Watts (BFW) potential to simulate a simple fluid. Our main aims are, firstly, to calculate the power exponents of pressure and energy as functions of strain rate, to examine if they have the same behavior as that of the Lennard-Jones fluid, and secondly, we wish to apply the combination of equilibrium MD and NEMD method developed in Chapter 6 to determine the BFW fluid-solid boundary, something which has not yet been determined.

The Barker-Fisher-Watts potential can be expressed by Eqn. (4.7). the parameters for argon are as follows in Table 7.1:

Table 7.1 Parameters for the BFW potential for argon [Bar71].

$\varepsilon/k(K)$	142.095
$\sigma(\text{\AA})$	3.3605
$r_m(\text{\AA})$	3.7612
A_0	0.27783
A_1	-4.50431
A_2	-8.331215
A_3	-25.2696
A_4	-102.0195
A_5	-113.25
C_6	1.10727
C_8	0.16971325
C_{10}	0.013611
α	12.5
δ	0.01

The parameters of the BFW potential are obtained by fitting the potential to experimental data such as molecular beam scattering, second virial coefficients, and long-rang interaction coefficients [Bar71]. σ is the distance where the potential is zero and is usually defined as the atomic diameter.

The Barker-Fisher-Watts (BFW) potential is an accurate two-body potential. In conjunction with an accurate three-body potential, it can be used to accurately describe a class of rare gases [Bar71]. It is different from the Lennard-Jones potential in that the Lennard-Jones potential is an effective potential which includes the effects of multi-body interaction. The

Lennard-Jones potential therefore can be applied to many kinds of atomic and molecular systems. The BFW potential, however, can only be used for certain types of molecules.

In this chapter we still adopt the usual convention for reduced units as in previous chapters, and we omit the asterisk in what follows.

7.1 The exponent

First, we presume that in planar Couette flow, the relationship between pressure or energy and strain rate can be expressed as Eqn. (5.19). In this equation, p_0 , E_0 are the equilibrium pressure and energy respectively. a and b are coefficients which depend on state point but do not depend on strain rate $\dot{\gamma}$. The power exponent α is not a fixed value, but should be determined by simulation. At each state point (T, ρ) , we use the following strain rates: $\dot{\gamma} = 0, 0.1, 0.2, 0.3, \dots, 0.6$. Our nonequilibrium molecular dynamics simulations use the SLLOD equations of motion with a Gaussian thermostat. The cut off distance is 4, and $\tau = 0.001$. We typically first run 50,000 time steps, do not use the results but use the configuration, then continue running about $10 \times 200,000$ time steps as production run. More details can be referred to the previous chapters.

In Figure 7.1 we plot pressure as a function of strain rate for the BFW fluid at a temperature and density of 0.85 and 0.84 respectively. Clearly the pressure has the expected power law behaviour, as is the case for all other state points studied here.

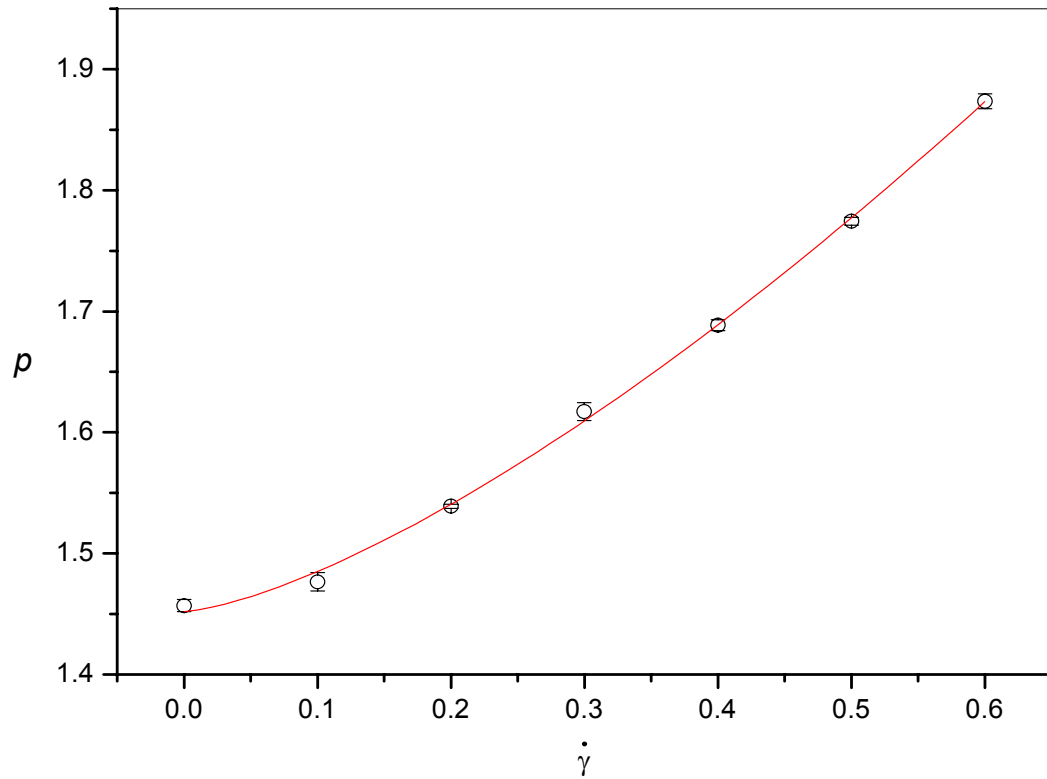


Figure 7.1 Pressure vs. strain rate for the BFW fluid at $(T, \rho) = (0.85, 0.84)$.

In Figure 7.2 we plot α as a function of ρ for three temperatures for both pressure and energy. From this plot, we can see that, for a certain temperature, the data points are basically along a straight line. This means that, similar to the Lennard-Jones fluid, the exponents of pressure and energy of the BFW fluid have a linear behaviour. The average error for the exponent fitting here is 0.046. Compared with the average error of exponent 0.022 for the Lennard-Jones fluid, our BFW simulations have larger errors.

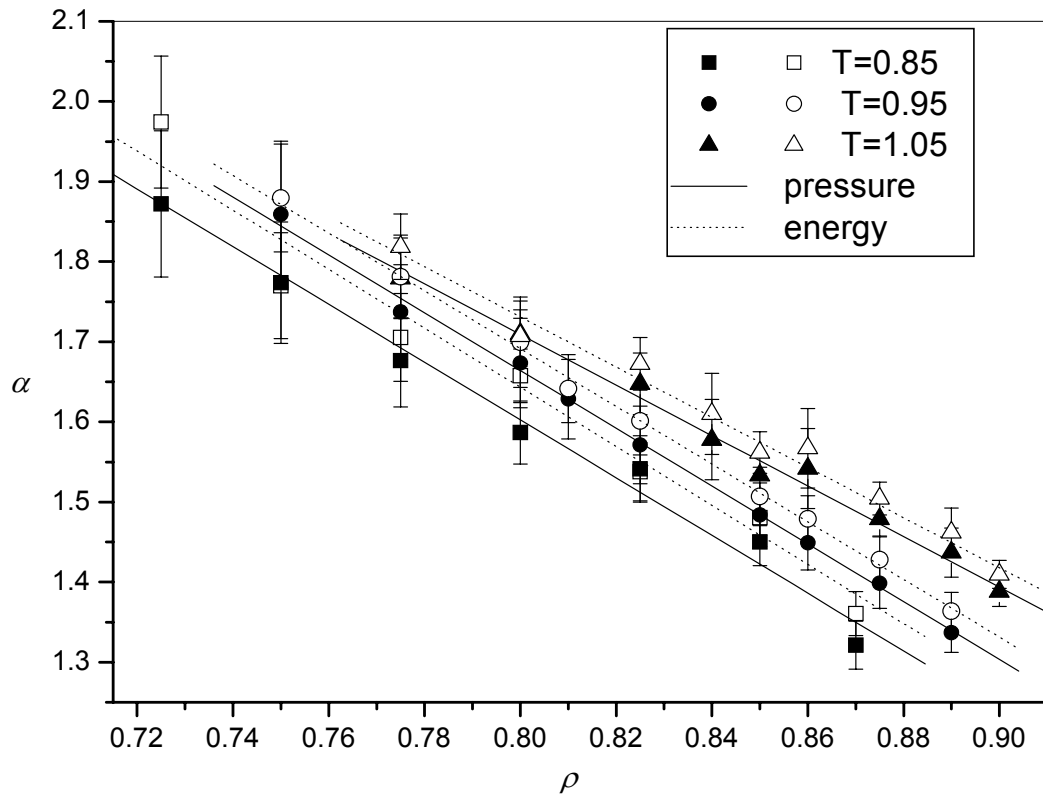


Figure 7.2 Exponents as a function of density at three temperatures. The solid symbols are exponents obtained from the pressure and the hollow symbols are obtained from the energy.

In Figure 7.3 we plot α for the pressure and energy at a fixed density of $\rho = 0.85$, and varying temperature. Although not very accurate, we still can recognize the plots as linear functions, as with the Lennard-Jones fluid. Deviations from linearity are most likely due to the much large statistical errors.

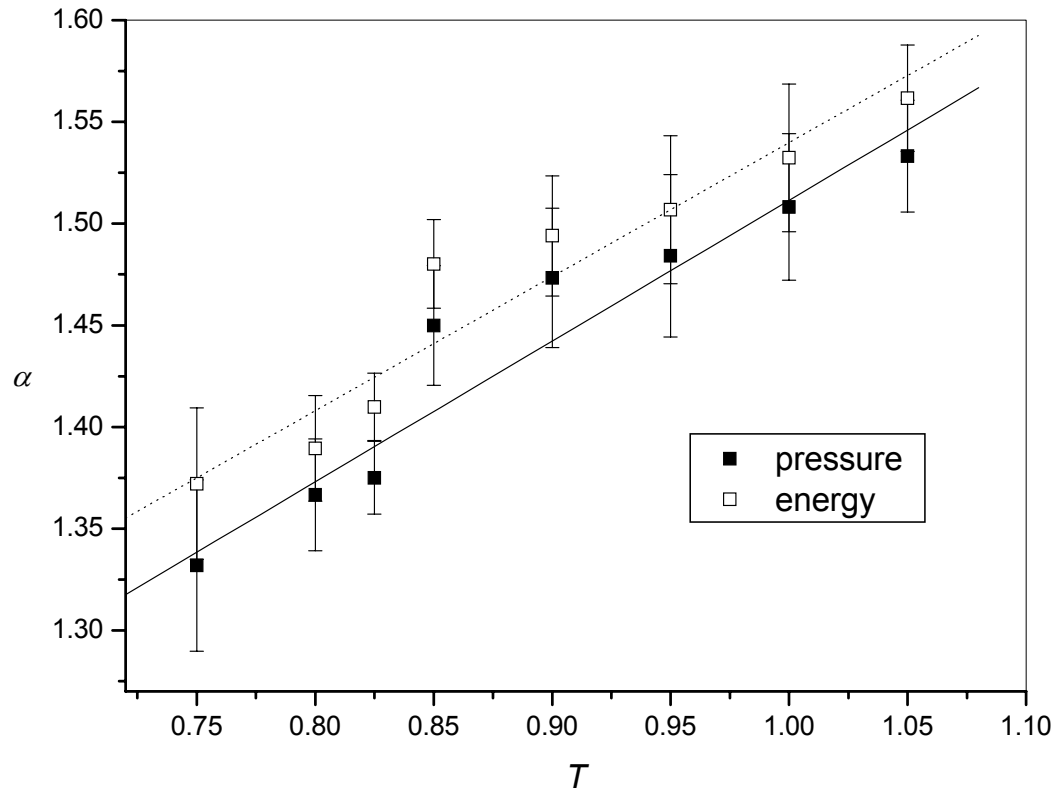


Figure 7.3 Exponents as a function of temperature at a density $\rho = 0.85$.

From Figures 7.2 and 7.3, we observe that the exponents appear to vary with both density and temperature linearly. If we assume that the exponents can be expressed as a linear function of both temperature and density, as with the Lennard-Jones fluid, then using all the simulation data, we find

$$\alpha = A + BT - C\rho \quad (7.1)$$

where $A = 3.80 \pm 0.14$, $B = 0.68 \pm 0.04$ and $C = 3.46 \pm 0.12$.

Comparing the above results and that of the corresponding coefficients of the Lennard-Jones fluid in Chapter 5, we can conclude that the exponent of the Barker-Fisher-Watts fluid has the same behaviour as that of the Lennard-Jones fluid. The exponent is not a fixed

value, $3/2$ or 2 , but changes continuously with state point in a linear manner. Furthermore, within errors, the coefficients are the same as that of the Lennard-Jones fluid. This can be seen from the Table 7.2.

Table 7.2 Comparison between the coefficients of the linear function for the LJ and BFW potentials.

	LJ	BFW
A	3.67 ± 0.04	3.80 ± 0.14
B	0.69 ± 0.03	0.68 ± 0.04
C	3.35 ± 0.03	3.46 ± 0.12

Here we should point out that because running the BFW program takes much more time than the Lennard-Jones program (more than 4 times longer), we did not run it for as long as the LJ program. Our results therefore have larger error bars.

7.2 Fluid-Solid Boundary

Next, we use the combination of equilibrium MD and NEMD to determine the fluid-solid boundary of BFW fluid. The details of this method are as described in Chapter 6.

In our work to determine the BFW fluid-solid boundary, we perform the following steps. First, at a trial state point, we conduct nonequilibrium dynamics simulation at only $\dot{\gamma} = 0$ and $\dot{\gamma} = 0.1$ to observe the first drop or gap in pressure, so we can determine which phase the state point belongs to. By doing this we can narrow our searching area quickly. Secondly, we use equilibrium MD to home into the freezing density. Third, at the freezing density we use pressure values at $\dot{\gamma} = 0.1, 0.3, \text{ and } 0.5$ to extrapolate the pressure to $\dot{\gamma} = 0$. Then, we use only three or four densities to construct part of the solid branch of the

equation of state (pressure-density curve). Finally, we draw a tie line from the freezing point on the liquid branch to the solid branch of the equation of state, and obtain the melting density. Our results are plotted in. Table 7.3.

Table 7.3 Fluid-solid boundary density at four temperatures.

T	0.75	0.85	0.95	1.05
ρ_f	0.877	0.896	0.908	0.931
ρ_s	0.976	0.986	0.994	1.012

We plot the fluid-solid boundary with the gas-liquid line taken from reference [Mar99] in Figure. 7.4. By extending the freezing line and right branch of gas-liquid line, we can find their intersection. We are therefore able to estimate the triple point of the BFW potential at $(T, \rho) = (0.5635, 0.8438)$. Because we do not have enough data points close to the intersection, the above estimation of the triple point is rather coarse.

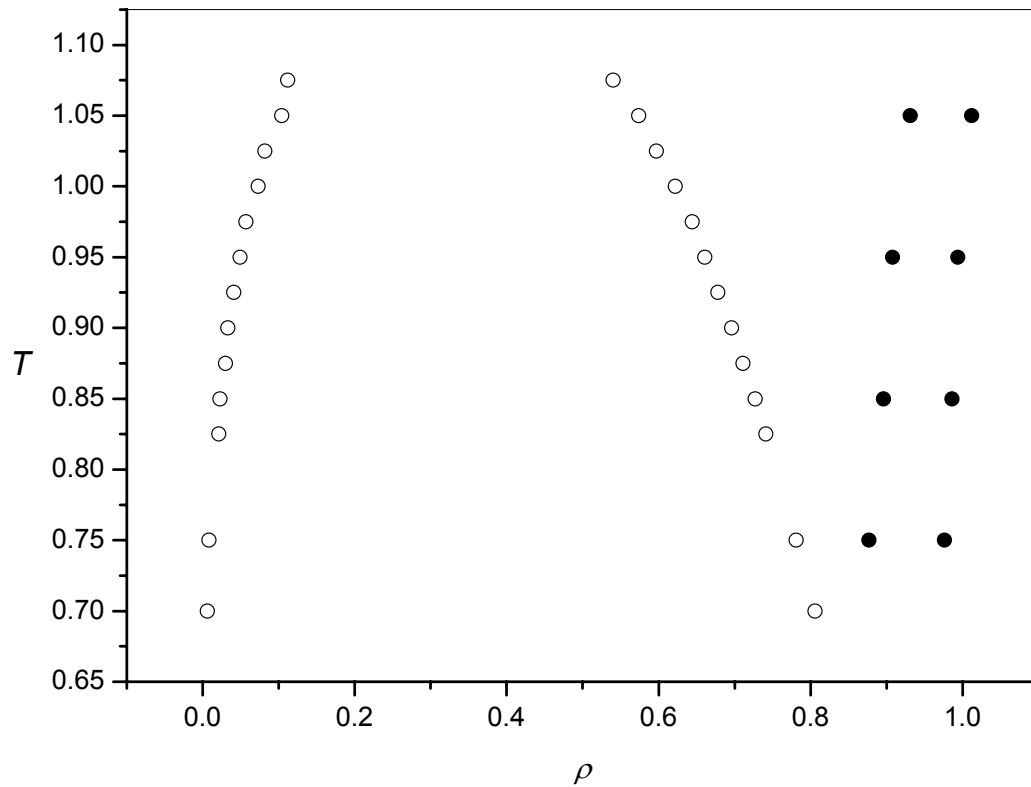


Figure 7.4 BFW phase diagram. Fluid-solid boundary denoted by solid symbols is obtained from our work. Gas-liquid boundary denoted by hollow symbols is from reference [Mar99].

As far as we know, there is no other published result about the BFW fluid-solid boundary, and there are two reasons for this. First, the BFW potential is much more complicated than the Lennard-Jones potential so it needs much longer simulation times to get the boundary data. Second, the results of the BFW potential cannot be compared with experiments on its own. It needs the inclusion of many-body effects. But our results still have significance, because the two-body potential dominates the material behaviour of the fluid, and it sets a basis for further work to include many-body effects. We did not have the time available to include these many body effects for this thesis, but leave it for future work.